M = cation
n = any species
NV = nonvolatile species
0 = on $x = 0$ side of film
ref = reference species

Superscripts

0 = infinite dilution
^ = a dimensional variable or parameter

LITERATURE CITED

Aul, E. F., R. D. Delleney, G. D. Brown, G. C. Page and D. O. Stuebner, "Evaluation of Regenerable Flue Gas Desulfurization Processes," *EPRI FP-272*, Vols. I, II (Jan., 1977).

Bourne, D. W., T. Higuchi and I. H. Pitman, "Chemical Equilibria in Solutions of Bisulphite Salts," *J. Pharm. Sci.*, **63**, 865-8 (1974).

Corbett, W. E., O. W. Hargrove and R. S. Merrill, "A Summary of the Effects of Important Chemical Variables upon the Performance of Lime/Limestone Wet Scrubbing Systems," EPRI FP-639 (Dec., 1977).

Eigen, M., K. Kustin and G. Maass, "Die Geschwindigkeit der Hydratation von SO_2 in wäßriger Lösung," *Z. Phys. Chem.*, **30**, 130-36 (1961).

Fuoss, R. M., "Ionic Association III. The Equilibrium Between Ion Pairs and Free Ions," *J. Am. Chem. Soc.*, **80**, 5059-61 (1958).

Gleason, R. J., and F. Heacock, "Limestone Wet Scrubbing of Sulfur Dioxide from Power Generation Flue Gas for High and Low Sulfur Fuels," *Adv. Chem. Ser.*, No. 127, 152-60 (1973).

Goddard, J. D., J. S. Schultz and R. J. Bassett, "On Membrane Diffusion with Near-equilibrium Reaction," *Chem. Eng. Sci.*, **25**, 665-83 (1970).

Hetherington, P. J., "Absorption of Sulfur Dioxide into Aqueous Media," Ph.D. thesis, Univ. Tasmania, Hobart (1968).

Hikita, H., S. Asai, T. Tsuji, "Absorption of SO_2 into Aqueous Sodium Hydroxide and Sodium Sulphite Solutions," *AIChE J.*, **23**, 538-44 (1977).

Hikita, H., S. Asai and H. Nose, "Absorption of Sulfur Dioxide in Water," *ibid.*, **24**, 147-9 (1978).

Husar, R. B., ed., "Sulfur in the Atmosphere," *Atoms. Env.*, **12** 1-796 (1978).

Huss, A., and C. A. Eckert, "Equilibria and Ion Activities in Aqueous Sulfur Dioxide Solutions," *J. Phys. Chem.*, **81**, 2268-70 (1977).

Kreuzer, F., and L. J. C. Hoofd, "Factors Influencing Facilitated Diffusion of Oxygen in the Presence of Hemoglobin and Myoglobin," *Resp. Phys.*, **15**, 104-24 (1972).

Kuehne, D. L., "Selective Transport of Sulfur Dioxide Through Polymer Membranes," Ph.D. thesis, Calif. Inst. Technol., (1979).

MacInnes, D. A., T. Shedlovsky and L. G. Longsworth, "The Limiting Conductances of Several Univalent Ions in Water at 25°," *J. Am. Chem. Soc.*, **54**, 2758-62 (1932).

Matson, S. L., C. S. Herrick and W. J. Ward, "Progress of the Selective Removal of H_2S from Gasified Coal Using an Immobilized Liquid Membrane," *Ind. Eng. Chem. Process Design Develop.*, **16**, 370-4 (1977).

McMichael, W. J., L. S. Fan and C. Y. Wen, "Analysis of Sulfur Dioxide Wet Limestone Scrubbing Data from Pilot Plant Spray and TCA Scrubbers," *ibid.*, **15**, 459-67 (1976).

Meldon, J. M., K. A. Smith and C. K. Colton, "An Analysis of Electrical Effects Induced by Carbon Dioxide Transport in Alkaline Solutions," in *Recent Developments in Separation Science*, CRC Press, Cleveland, Ohio (1979).

Moelwyn-Hughes, E. A., *The Chemical Statics and Kinetics of Solutions*, Academic Press, New York, (1971).

Nernst, W., "Zur Kinetik der nin Lösung Besindlichen Körper," *Zeit. Phys. Chem. (Leipzig)*, **2**, 613-37 (1888).

Newman, J. S., *Electrochemical Systems*, Prentice-Hall, Englewood Cliffs, N. J. (1973).

Onda, K., T. Kobayashi, M. Fujine and M. Takahashi, "Behavior of the Reaction Plane Movement in Gas Absorption Accompanied by Instantaneous Chemical Reactions," *Chem. Eng. Sci.*, **26**, 2009-26, 2027-35 (1971).

Roberts, D. L., "Sulfur Dioxide Transport Through Aqueous Solutions," Ph.D. thesis, Calif. Inst. Technol. (1979).

Rochelle, G. T., and C. J. King, "The Effect of Additives on Mass Transfer in $CaCO_3$ or CaO Slurry Scrubbing of SO_2 from Waste Gases," *Ind. Eng. Chem. Fundamentals*, **16**, 67-75 (1977).

Rowland, C. H., and A. H. Abdulsattar, "Equilibria for Magnesia Wet Scrubbing of Gases Containing Sulfur Dioxide," *Env. Sci. Tech.*, **12**, 1158-62 (1978).

Schultz, J. S., J. D. Goddard and S. R. Suchdeo, "Facilitated Transport via Carrier-Mediated Diffusion in Membranes," *AIChE J*, **20**, 417-45; 625-45 (1974).

Sherwood, T. K., R. L. Pigford, and C. R. Wilke, *Mass Transfer*, McGraw-Hill, New York, (1975).

Tartar, H. V., and H. H. Garretson, "The Thermodynamic Ionization Constants of Sulfurous Acid at 25°C," *J. Am. Chem. Soc.*, **63**, 808-16 (1941).

Wang, J. C., and D. M. Himmelblau, "A Kinetic Study of Sulfur Dioxide in Aqueous Solution with Radioactive Tracer," *AIChE J*, **10**, 574-80 (1964).

Ward, W. J., "Immobilized Liquid Membranes," in *Recent Developments in Separation Science*, CRC Press, Cleveland, Ohio, (1972).

Zavaleta, R., and F. P. McCandless, "Selective Permeation through Modified Polyvinylidene Fluoride Membranes," *J. Mem. Sci.*, **1**, 333 (1976).

Manuscript received March 12, 1979; revision received January 17, and accepted January 23, 1980.

Part II. Experimental Results and Comparison with Theory

Measurements were made of the steady state flux of sulfur dioxide through films of water and solutions of neutral and alkaline sodium salts (0.1 to 2.0M sodium chloride, 10^{-3} to 3.0M sodium hydroxide, $NaHSO_3$ or sodium sulfite) with sulfur dioxide partial pressures between 10 and 100Pa. In agreement with equilibrium theory (Part I), data from water and sodium chloride solutions show that HSO_3^- is responsible for 83 to 95% of the flux (facilitation factor F between 5 and 19). In alkaline solutions, HSO_3^- and other sulfur containing species cause F to be as large as 1 370. Equilibrium theory, however, overpredicts F by up to a factor of 7. The NEBLA (Part I) accounts for this deviation.

SCOPE

Interest in flue gas desulfurization (FGD) has given rise to a number of fundamental studies on the absorption of sulfur dioxide into water (Hikita et al., 1978) and into sodium hydroxide, $NaHSO_3$, and sodium sulfite solutions (Hikita et al., 1977; Takeuchi et al., 1975; Onda et al., 1971; Hetherington, 1968; Goettler, 1967). With the exception of Takeuchi et al., pure sulfur dioxide was absorbed so that partial pressures of interest in FGD (approximately 10 to 100Pa) were not studied. At the low partial pressures typical of FGD, the sulfur containing ions formed by the reactions of sulfur dioxide in solution are a much

0001-1541-80-3357-0602-$01.05.

larger fraction of the total dissolved sulfur. Hence, from the standpoint of applications and of understanding the transport mechanism, experiments with low partial pressures of sulfur dioxide are desirable.

In this study, experiments are performed with films of water and solutions of sodium chloride, sodium hydroxide, and sodium sulfite with sulfur dioxide partial pressures of 10, 20, 50 and 100Pa. These partial pressures and the concentrations of alkaline salts are typical of FGD applications. The aqueous films, in the form of agar gels or soaked polyethylene filters, were mounted in a diffusion cell. Humidified nitrogen with a known mole fraction of sulfur dioxide flowed through one side of the cell. Clean, humidified nitrogen flowed through the other side, sweeping away sulfur dioxide passing through the films. Measurement of the sulfur dioxide concentration in this stream determined the rate at which sulfur dioxide was passing through the films. Data are compared with both the equilibrium and nonequilibrium (NEBLA) theories developed in Part I.

CONCLUSIONS AND SIGNIFICANCE

Data taken with water and 0.1 to 2.0M sodium chloride agree well with the equilibrium theory developed in Part I. This agreement indicates that the reaction of sulfur dioxide (aq) with water is fast, that the potential gradient is an essential part of the theory and that HSO_3^- dominates the flux ($5 < F < 19$). The data allow a lower limit to be set on the rate coefficient k_1 that indicates that the value of k_1 given by Eigen et al. (1961) should be accepted until further rate measurements are made.

The main difference between neutral salt solutions and water is the ionic strength which can cause activity coefficients to become important. For sodium chloride solutions, the γ_i model proposed by Bromley (1972) is found to be adequate. For $I \geq 0.5$M, choice of a γ_i model can affect the flux prediction by a factor of 2 or more.

The flux through alkaline solutions (10^{-3}M $\leq Na_{tot} \leq$ 3.0M) is found to be up to a factor of 28 higher than through water. Although this increase is significant, it is a factor of 7 lower than the prediction of equilibrium theory. A singular perturbation analysis adapted from Schultz et al. (1974) also overpredicts the flux. The NEBLA developed in Part I agrees with most of the data to within 30%. The observed facilitation factors are large (up to 1 370) so that the sulfur dioxide/alkaline salt system lies far from the limits of instantaneous and slow chemical reactions. In this sense, the NEBLA succeeds in the intermediate kinetic regime that has not been covered successfully by previous analyses that rely on a perturbation from the limit of either fast or slow reactions.

The boundary layer at x = 0 is negligible, and it is the boundary layer at x = 1 that is responsible for the factor of 7 deviation from equilibrium. The NEBLA calculations show that δ_1 is approximately 0.1% of the film thickness. Because the films are 1mm thick, $\delta \simeq 1\mu$m. Data with different film thicknesses ($0.37 \leq L \leq 4.8$mm) show that the deviation from equilibrium increases and that δ_1 increases as L decreases, in qualitative agreement with the NEBLA.

When applied to water, the NEBLA predicts both boundary layer resistances to be negligible and agrees with the water data and equilibrium theory to within 10%. The ability of the NEBLA to predict the flux accurately in the equilibrium limit and far from the equilibrium limit is a result of the pH dependence of δ_1. Because of this wide range of applicability in the sulfur dioxide system, the approach of the NEBLA is recommended for other facilitated transport systems.

EXPERIMENTAL SYSTEM

Measurements of the steady state flux of sulfur dioxide through aqueous films of known composition were made with the apparatus shown in Figure 1. The aqueous film under study divided the cell into two halves. Nitrogen flowing to each half of the cell was humidified by passing through gas washing bubblers. A resistance heating tape warmed the first bubbler in each line enough to cause condensation between the bubblers. Gas leaving the second bubbler was thereby saturated at room temperature.

The humidified gas on the upstream side of the cell passed through a tee where sulfur dioxide was added through a double-pattern needle valve. This sulfur dioxide flow, adjusted to give a desired $y_{SO_2,0}$, was measured by an electronic mass flow meter. The output of the mass flow meter (MFM) was read in volts on a digital panel meter (DPM).

This humidified nitrogen and sulfur dioxide stream continually flowed through the upstream side of the cell, exposing the aqueous film to the desired $y_{SO_2,0}$. Less than 1% of the sulfur dioxide entering the cell dissolved in the aqueous film, reacted and diffused to the other side of the film. Here, a clean, humidified nitrogen stream entered the cell and carried away the sulfur dioxide coming through the film.

A flame-photometric detector (FPD) determined the sulfur dioxide mole fraction in the gas stream leaving the downstream side of the cell ($y_{SO_2,1}$). The oxygen required for operation of the analyzer was added downstream of the cell to avoid oxidation of sulfur dioxide to $SO_4^=$ in the aqueous film. Teflon lines carried the downstream flow because the low (~0.1 ppm) sulfur dioxide concentrations in this stream were susceptible to absorption losses.

Gases from both sides of the cell exhausted to a hood through 0.79 cm ID polyethylene or teflon tubing. The pressure drop was small, and the cell was near atmospheric pressure (99 to 100 kPa). The cell operated at room temperature (297° to 299°K).

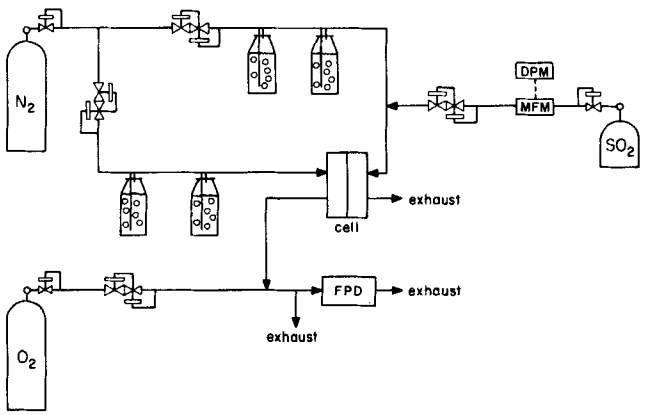

Figure 1. Apparatus. The aqueous film is held in the cell. Nitrogen, humidified to prevent evaporation of the film, carries sulfur dioxide to one side of the cell. A clean nitrogen stream sweeps away sulfur dioxide that passes through the film and the flame-photometric detector (FPD) measures the concentration of sulfur dioxide in the sweep stream.

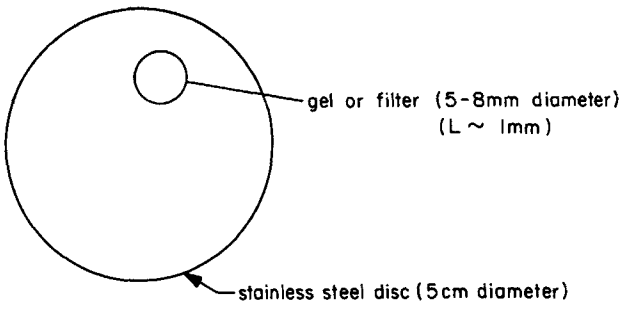

Figure 2. Aqueous film support. Gel or filter in off centered hole in stainless steel disk. The film thickness is 1 ± 0.1 mm in most experiments.

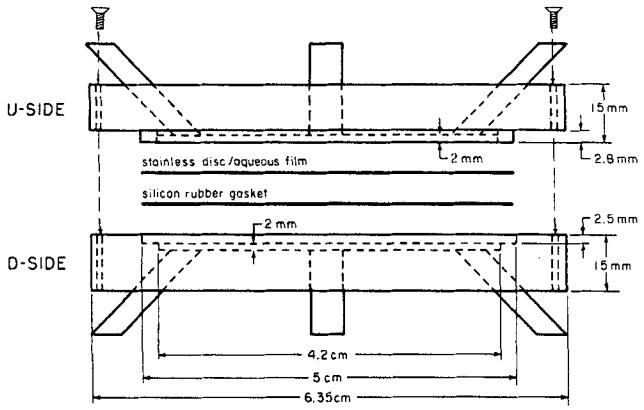

Figure 3. Cell design. The stainless disk holding the aqueous film rests on a silicon rubber gasket which is placed on the lip of the D side. When the cell is closed, there is a 2 mm deep gas chamber above and below the aqueous film. Gases flow into and exhaust from these chambers. Inlet ports are positioned to cause swirl.

Measurements and Calibrations

Data for calculating the flux of sulfur dioxide and for comparing with theory include the cross-sectional area of the aqueous film A, the film thickness L, the mole fraction of sulfur dioxide in the stream sampled by the FPD, y_m, and four flow rates: 1), 2) the humidified nitrogen streams going to the upstream and downstream sides of the cell, 3) the oxygen stream and 4) the sulfur dioxide added to the nitrogen flow to the upstream side of the cell.

The analogue output of the FPD indicated y_m. The FPD was calibrated by passing a sulfur free air stream at a known flow rate over a sulfur dioxide permeation tube (1 cm, low emission) and into the analyzer. The tube was weighed every 2 wk on a microbalance to determine its sulfur dioxide emission rate.

The nitrogen and oxygen flows were measured with a wet test meter before sulfur dioxide was allowed into the system. The nitrogen flows (M_u, M_d) were 3 to 6 l/min. The oxygen flow rate was set so that $M_{O_2}/M_d = 21/79$, simulating the atmospheric oxygen/nitrogen molar ratio. A 700 kPa pressure drop across each double-pattern needle valve stabilized these flow rates. No measurable change occurred during an experiment.

The wet test meter (WTM) was calibrated by displacing water from a 1 l volumetric flask. It was found that each revolution of the WTM represented only 2 916 cm^3 rather than the 3 000 cm^3 indicated on the face of the WTM. This meter factor of 0.972 was incorporated into all flow measurements.

A (linear) calibration curve gave the sulfur dioxide molar flow rate M_{SO_2} from the DPM volt reading. Calibration was done with a bubble flow meter (a 10 ml buret with 0.05 cm^3 divisions). To achieve equilibration of the sulfur dioxide with the soap solution used in the buret, sulfur dioxide was passed through the meter for one day before calibration data were taken.

Aqueous Film Preparation

The aqueous film was either a soaked filter or a gel and was held in a circular hole in a stainless steel disk (Figure 2). The cross-sectional area of the aqueous film was computed from the diameter of the hole (4.76 to 7.94 mm). The disk was type 316 stainless steel, 0.64 mm thick.

A soaked filter was used for studying concentrated sodium hydroxide solutions (≥0.5M). The filter material was porous ultrahigh molecular weight polyethylene (UHMW PE). Polyethylene is highly resistant to attack by inorganic neutral and alkaline salt solutions (Standen, 1962). Disks of 1 mm thickness and 4.76 mm diameter were cut from sheets of porous UHMW PE and inserted into the circular hole in the stainless disk.

Approximately 100 ml of solution were pulled through the disk with a slight aspirator suction to ensure saturation of the filter with the solution (100 ml is 1 000 times the void volume of the filter). A small amount of RTV silicone-rubber sealant was applied along the outer edge of the filter to hold it to the stainless steel.

The stainless steel disk and filter were put into the cell, and the experiment outlined above was performed. After the experiment, the filter was flushed with double-distilled water (~100 ml) and kept submerged in a closed petri dish. Hence, the filter was never dry, and air was not trapped in the filter interstices. The effects of the filter matrix on the flux were assumed to be geometric only (blocked surface area and tortuosity) and were accounted for by calibrating the filter (Roberts, 1979).

Agar gels were used for studying water, neutral salt solutions (0.1 to 2.0M sodium chloride) and alkaline salt solutions with $0.001M \leq Na_{tot} \leq 0.2M$. Gels were cast in the circular hole in the stainless disk. Immediately after the experiment, the stainless disk was taken to a balance where the gel was cut out with a surgical blade and weighed. This weight and the gel density gave the thickness of the gel (1 ± 0.1 mm).

Since the agar gel decreased the diffusivities of the species in the aqueous film, a 5% correction was made before data were compared with theory. This 5% correction was taken from Chilcote (1970) who measured diffusivities of Na^+ in 1% agar gels and compared them to values obtained in free aqueous solutions.

Cell Design

Figure 3 shows the cell configuration. The stainless disk holding the aqueous film was placed on top of a 0.794 mm thick rubber gasket that rested on a lip on the downstream side (D side). The upstream side (U side) was attached to the D side by six screws (type 6-32). Since the cell operated at room pressure, no special sealing precautions were needed.

TABLE 1. SUMMARY OF EXPERIMENTAL PROGRAM

Type of experiment	Purposes/questions addressed
Water*	Test of equilibrium theory ($d\Phi/dx$ included) Estimate k_1 for hydrolysis: $SO_2(aq) + 2H_2O \underset{k_{-1}}{\overset{k_1}{\rightleftarrows}} H_3O^+ + HSO_3^-$
Neutral salt* 0.1, 0.5, 1.0, 2.0M NaCl	Test activity coefficient model Effect of viscosity on diffusion coefficients Test effectiveness of $d\Phi/dx$ in a neutral salt
Alkaline salt* $NaOH/NaHSO_3/Na_2SO_3$ $Na_{tot} = 10^{-3}, 10^{-2}, 0.05, 0.2, 0.5, 1.0, 2.0, 3.0M$	Test for flux increase over water and for large facilitation factors Test equilibrium theory and NEBLA
Variable film thickness $Na_{tot} = 0.05M$ $y_{SO_2,0} = 2 \cdot 10^{-4}$ $0.37 \text{ mm} \leq L \leq 4.8 \text{ mm}$	Test variation of facilitation factor with film thickness predicted by NEBLA

* Gas phase SO_2 mole fractions $10^6 \cdot y_{SO_2,0} = 100, 200, 500, 1\,000$; $10^6 \cdot y_{SO_2,d} \simeq 0.1$.

Gases entered each side of the cell through two 6.35 mm OD tubes attached at 45 deg angles. These tubes were attached on opposite edges in such a way that a swirling motion of the gas in the cell was produced. Stagnant regions were thereby eliminated. Exhaust occurred through a centered 7.94 mm ID port. Except for a teflon exhaust port on the D side, the cell was 316 stainless steel.

Experimental Program

Table 1 gives the types and concentrations of solutions studied and the goals for each set of experiments. Fluxes were measured at each solution concentration for four different gas phase concentrations: $y_{SO_2,0} = 10^{-4}$, $2 \cdot 10^{-4}$, $5 \cdot 10^{-4}$ and 10^{-3}. The mole fraction $y_{SO_2,1}$ was held constant at 10^{-7} by adjusting M_d and by changing the diameter of the hole in the stainless disk that held the aqueous film. Except for the variable thickness studies, the film thickness was 1 ± 0.1 mm.

Three flux measurements were made at each salt concentration and each value of $y_{SO_2,0}$. Data and error bars in the next section are based on the average and scatter of the three runs.

RESULTS AND DISCUSSION

Water—Comparison with equilibrium theory

Equations (30) and (31) in Part I summarize the equilibrium theory for sulfur dioxide/water solutions. For the values of $y_{SO_2,0}$ and $y_{SO_2,1}$ in this study

$$\frac{y_{SO_2,0}^{\frac{1}{2}} - y_{SO_2,1}^{\frac{1}{2}}}{y_{SO_2,0} - y_{SO_2,1}} \simeq y_{SO_2,0}^{-\frac{1}{2}} \tag{1}$$

If we substitute the various coefficients (25°C) into Equation (31), Part I, and use the Davies model for activity coefficients (Davies, 1962), F_{eq} becomes

$$F_{eq} \simeq 0.18\, y_{SO_2,0}^{-\frac{1}{2}} \tag{2}$$

Figure 4 shows the data obtained with water/1% agar films of 1 mm thickness. The abscissa is $y_{SO_2,0}^{-\frac{1}{2}}$ so that Equation (2) is represented by a straight line. There are four data points at each value of $y_{SO_2,0}$ although some points coincide. Table 2 gives the average measured fluxes.

Equilibrium theory, Equation (2), falls close to the data, verifying the equilibrium approximation in this case, the necessity of including the potential gradient in the theory and the unimportance of sulfur containing ions other than HSO_3^-. As indicated by the facilitation factor, the HSO_3^- contribution to the flux is five to twenty times the sulfur dioxide (aq) contribution. In contrast, the HCO_3^- ion contributes little to the flux in the carbon dioxide/water system, where the hydrolysis

$$CO_2 + 2H_2O \rightleftarrows H_3O^+ + HCO_3^- \tag{3}$$

is much slower (Suchdeo and Schultz, 1974). Since the potential gradient increases the effective diffusivity of HSO_3^- by approximately 73%, and since HSO_3^- dominates the flux, the potential gradient is responsible for about 42% (0.73/1.73) of the flux.

Water—Estimate of k_1

Since the data support the equilibrium approximation, the hydrolysis of sulfur dioxide (aq) [Equation (37), Part I] must be fast. Therefore, the perturbation analysis given by Suchdeo and Schultz (1974) in their study of the transport of carbon dioxide in aqueous solutions applies to the sulfur dioxide/water system. This analysis (SS analysis) gives the facilitation factor F_{SS} as a function of the system parameters $y_{SO_2,0}$, $y_{SO_2,1}$, L, k_1, K_1, $\hat{D}_{SO_2}$, $\hat{D}_{HSO_3^-}$ and $\hat{P}_{tot}$. In contrast, the equilibrium theory [Equation (31), Part I] does not depend on k_1 or L.

The Damkohler number

$$Da = \frac{k_1 L^2}{\hat{D}_{SO_2}} \tag{4}$$

is the important nondimensional parameter that arises in the SS analysis. When Da is large enough, F_{SS} approaches the equilibrium value F_{eq}.

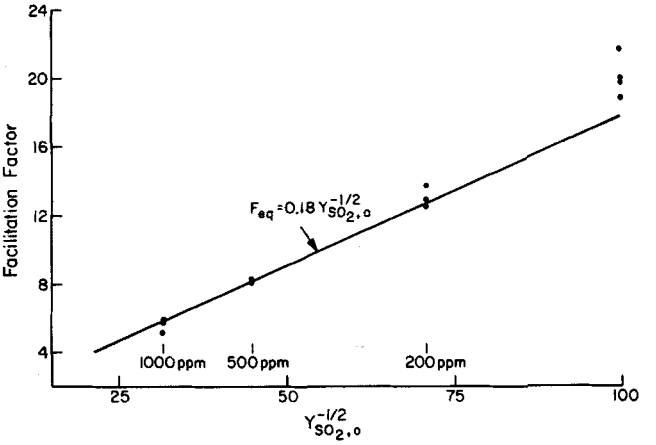

Figure 4. Water with 1% agar. Equilibrium theory, summarized by Equations (30) and (31), Part I, and (2), agrees with measurements of sulfur dioxide transport through water/1% agar films. The HSO_3^- ion dominates the transport.

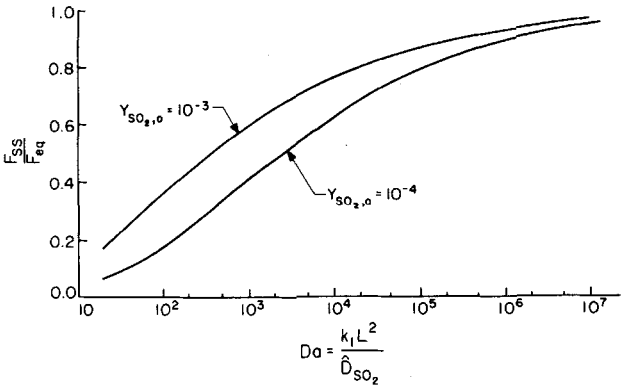

Figure 5. Damkohler number required to reach equilibrium limit. Analysis of Suchdeo and Schultz (1974) gives facilitation factor F_{SS} as a function of the Damkohler number. Equilibrium limit is reached when $F_{SS} = F_{eq}$. Estimate of k_1 is possible since water data are in equilibrium limit.

Figure 5 shows the graph of F_{SS}/F_{eq} vs. Da for $y_{SO_2,0} = 10^{-3}$ and 10^{-4}. The other values of $y_{SO_2,0}$ in this study lie between these curves. Since the sulfur dioxide/water data show $F = F_{eq}$, Figure 5 shows that the Damkohler number must be at least 10^5 to 10^6. As a conservative approximation

$$Da \geq 2 \cdot 10^5 \tag{5}$$

is chosen.

The gel thicknesses in the water studies were 1 mm. Given $L = 1$ mm and $\hat{D}_{SO_2} = 1.6 \cdot 10^{-5}$ cm^2 s^{-1}, Equation (5) implies

$$k_1 \geq 320 \text{ s}^{-1} \tag{6}$$

Equation (6) gives a lower limit on k_1 that is approximately 10^4 larger than reported by Wang and Himmelblau (1964). It also comes closer to substantiating Eigen's (1961) value than the other estimates of k_1 in the literature (Roberts, 1979, Table 2.4).

With a 1 mm film, the Damkohler number calculated from Wang and Himmelblau's, Phipps' (1947) and Eigen's values for k_1 are

$$Da_{WH} = 19.8 \tag{7}$$

$$Da_p = 2\,550 \tag{8}$$

$$Da_E = 3.1 \cdot 10^9 \tag{9}$$

The extent of disequilibrium implied by Equations (7) and (8) is apparent from Figure 5, although the perturbation analysis overestimates F_{SS} when $F_{SS} \lesssim 0.6 F_{eq}$. Eigen's k_1 value lies in the equilibrium limit (off the graph). This value ($k_1 = 5 \cdot 10^6$ s^{-1} at 25°C) will be used in the remainder of this study.

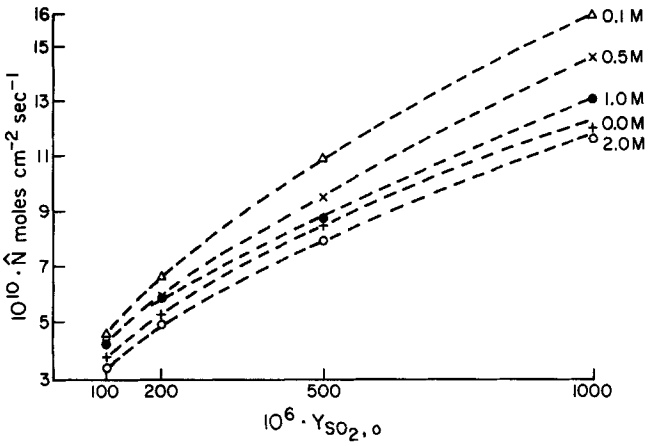

Figure 6. Sodium chloride and water data. In dilute concentrations, sodium chloride salts in the HSO_3^- ion so that the flux is higher than through water (0.0M). Continued increase in sodium chloride concentration increases solution viscosity and reduces salting in effect. Flux for 2.0M sodium chloride falls below water data.

Neutral Salt Solutions—Sodium Chloride

Two effects of increasing sodium chloride concentrations are apparent in Figure 6 where the complete range of sodium chloride data are shown with the sulfur dioxide/water data (Table 2). First, the flux through 0.1M sodium chloride solutions is approximately 40% larger than through water films. This increase, which corresponds to an increase in the equilibrium concentration of HSO_3^-, results from the tendency of ions to stabilize each other at low enough ionic strengths (salting in

TABLE 2

Flux of SO_2 through Water/1% agar films

$10^6 \cdot y_{SO_2,o}$	$10^{10} \cdot \hat{N}$ $\frac{\text{moles}}{\text{cm}^2\text{s}}$
100	3.81 ± 0.17
200	5.32 ± 0.37
500	8.44 ± 0.08
1 000	11.9 ± 0.72

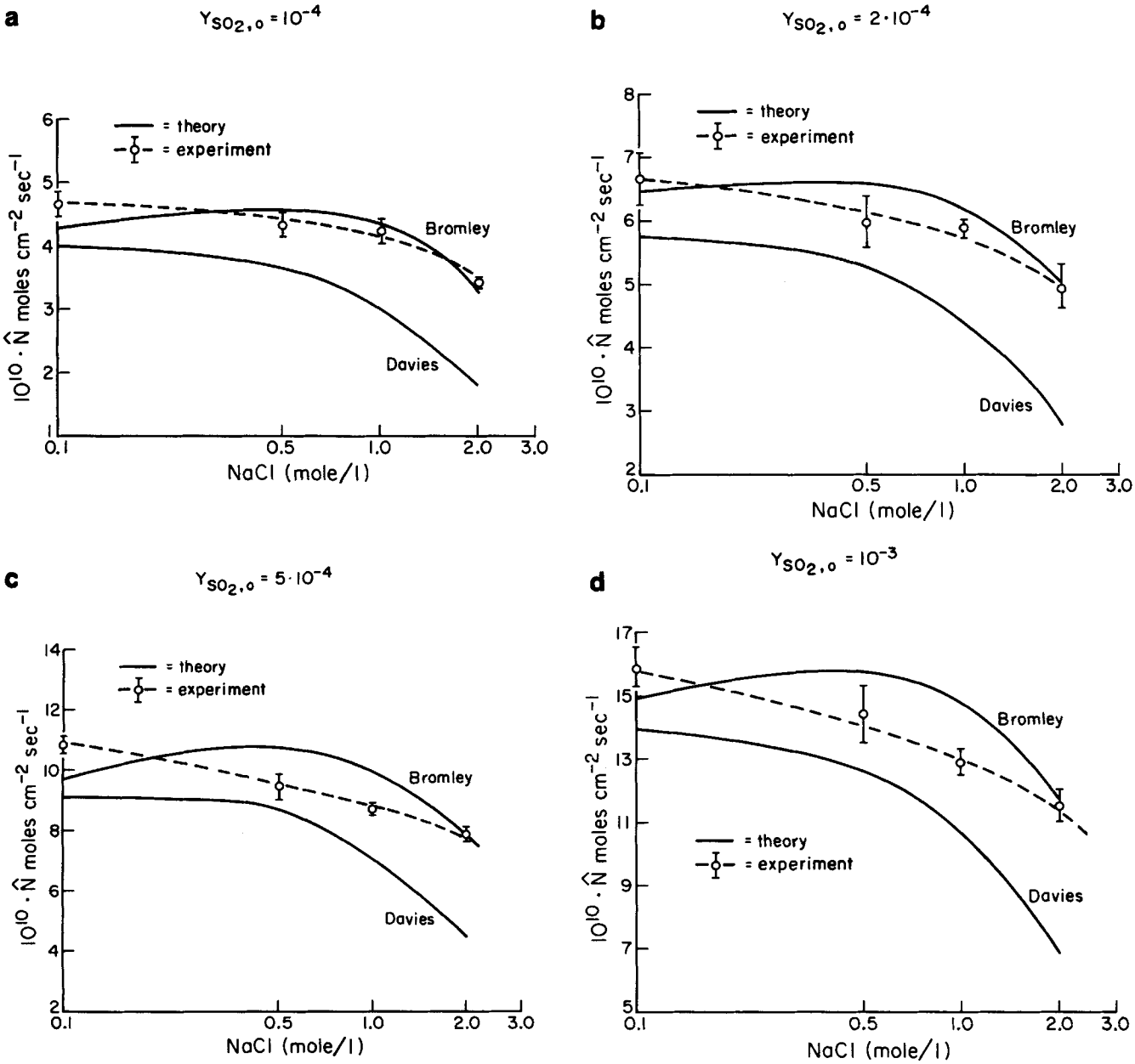

Figure 7a to d. These four figures compare the sodium chloride data with the equilibrium theory [Equation (30), Part I] using both the Bromley and Davies activity coefficient models. Each figure is for a different value of $y_{SO_2,o}$ (10^{-4}, $2 \cdot 10^{-4}$, $5 \cdot 10^{-4}$ and 10^{-3}). The comparison shows that the equilibrium theory succeeds and that Bromley's model is preferable in sodium chloride solutions.

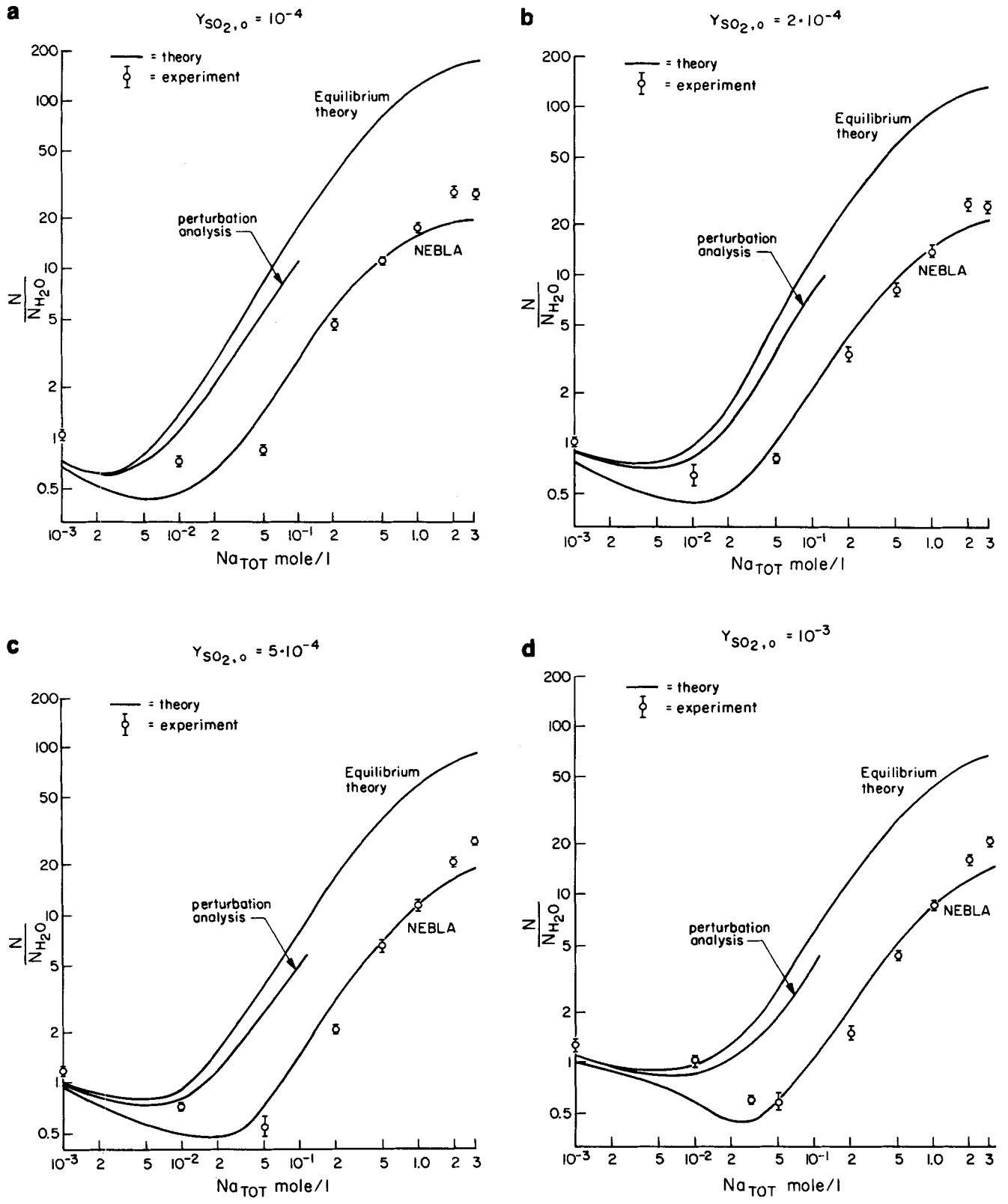

Figures 8*a* to *d*. Alkaline solution data for $y_{SO_2,0} = 10^{-4}, 2 \cdot 10^{-4}, 5 \cdot 10^{-4}$ and 10^{-3} are presented in these four figures. Alkaline sodium increases the flux by up to a factor of 28 over water. Equilibrium theory, a perturbation analysis adapted from Schultz et al. (1974), and the NEBLA are compared with the data. When $NA_{tot} > 0.03M$, the equilibrium and perturbation theories overpredict the flux by up to a factor of7; the NEBLA is within 30%. Below 0.03M, the theory does not account properly for the potential gradient and underestimates the flux.

effect). This effect is directly related to the minimum in the activity coefficient curve that exists near I = 0.1M for most species.

The second effect is the decrease in the flux that results from the increased solution viscosity at higher sodium chloride concentrations. Also, the salting in of HSO_3^- becomes less effective as the sodium chloride concentration increases. The increased solution viscosity reduces the flux at 2M to a value below the water data.

In Figures 7*a* to *d*, the sodium chloride data are compared

TABLE 3. FACILITATION FACTORS FROM ALKALINE SOLUTION DATA

Na_{tot} mole/l	$10^6 \cdot y_{SO_2,0}$ 1 000	500	200	100
0.0	5.73	8.73	13.8	19.7
10^{-3}	6.86	9.60	14.7	21.2
10^{-2}	6.04	5.86	8.42	13.4
0.05	2.65	3.80	10.8	15.6
0.20	8.62	17.9	52.3	103
0.50	31.3	65.9	132	261
1.0	73.0	133	267	476
2.0	175	321	661	997
3.0	305	573	878	1 370

with the equilibrium theory [Equation (30), Part I]. Both the Davies and Bromley activity coefficient models are tested. The results show that the equilibrium theory works in concentrated neutral solutions. The potential gradient, included in the equilibrium theory, is necessary for proper modeling of the system, even in concentrated solutions. The approximate method of accounting for the potential gradient (Part I) appears to be valid.

Bromley's activity coefficient model is preferable in sodium chloride solutions. In the most concentrated solutions, the Davies model deviates from the data by a factor of 2, while Bromley's model agrees well with the data. One might expect Bromley's model to be more accurate in sodium chloride solutions because it has been used successfully for seawater. Davies' model is based on data for many solutions.

When the concentration is less than 0.5M, however, the Bromley theory is not significantly closer to the data than the Davies theory. The neutral salt data therefore show that for $I \leq 0.5$M, a simple model (Davies') works as well as a complex model (Bromley's). This observation allows the Davies model to be used for other aqueous sulfur dioxide solutions when $I \leq 0.5$M. The relative simplicity of the Davies model is an advantage in making calculations.

Some test other than the sodium chloride experiments must be made to obtain an activity coefficient model for the alkaline solutions when $Na_{tot} \geq 0.5$M. For this purpose, Roberts (1979, Appendix C) compared the equilibrium solubility of sulfur dioxide in alkaline sodium solutions computed using Davies' activity coefficient model with the solubility data of Johnstone and Blankmeyer (1938). Agreement was excellent (within 10%). Therefore, the Davies model was used in calculations for alkaline solutions in the present study.

Alkaline Solutions—Sodium Hydroxide/$NaHSO_3$/Sodium Sulfite

Alkaline solutions with the same total sodium concentration will behave the same at steady state when the alkaline salts that are used have no anions that are foreign to the sulfur dioxide/water system. The following results, therefore, apply to any mixture of sodium hydroxide, $NaHSO_3$, sodium sulfite or $Na_2S_2O_5$.

All theoretical calculations for alkaline solutions are made with the chemical speciation and the various measured and estimated equilibrium and diffusion coefficients discussed in Part I, the Davies γ_i model and the Stokes-Einstein dependence of D_i on μ. Viscosity is taken to be that of a sodium hydroxide solution with the same Na_{tot} concentration. This approximation is reasonable, since viscosities of sodium hydroxide, $Na_2S_2O_3$ and sodium sulfate solutions with the same Na_{tot} differ by only a few per cent (Weast, 1971).

General Results: Figures 8*a* to *d* show the alkaline solution data for $y_{SO_2,0} = 100$, 200, 500 and 1 000 ppm. The film thickness is 1 mm. Also shown are the equilibrium theory (Part I), the NEBLA (Part I) and a perturbation solution adapted from Schultz et al. (1974).

Adding alkaline salts to the solution has a significant effect, since N/N_{H_2O} ranges up to 28. The intuitive notion that alkaline solutions increase the sulfur dioxide transport rate is verified. The minimum in the curve, however, was not expected and will be discussed later.

For $Na_{tot} \geq 0.03$M, the equilibrium theory overestimates the flux by about a factor of 7. The equilibrium approximation, therefore, is invalid in some aqueous sulfur dioxide solutions. It is necessary to quantify what is meant by instantaneous before the equilibrium approximation can be used confidently.

The singular perturbation analysis adapted from Schultz et al. (1974) overpredicts the data also. This analysis is valid in the limit of fast reactions and is not intended to predict a factor of 7 deviation from equilibrium. It is included to show that existing perturbation analyses do not apply to the present system because it is far from equilibrium.

For $Na_{tot} \geq 0.05$M, the NEBLA predicts the data with a maximum deviation of 30%. When $Na_{tot} < 0.05$M, the approximate method of accounting from the potential gradient causes the theory to underpredict the data by up to 50%. The deviation of a maximum of 30% must be viewed as excellent when the approximations in the NEBLA are considered.

Table 3 shows the facilitation factors calculated from the data in Figures 8*a* to *d*. These values of F are up to 450 times larger than those observed in previous sulfur dioxide transport studies. The sulfur containing ions dominate the flux. In the equilibrium core, sulfur dioxide (aq) carries a small fraction of the flux [approximately $1/(F + 1)$]. Because F is large, the system lies far from the limit of zero chemical reactions. The sulfur dioxide/alkaline salt system, therefore, lies far from the limits of both instantaneous and slow chemical reactions.

Characteristics of the NEBLA*; Definition of Instantaneous:* Reactions in the sulfur dioxide system are considered fast by most standards, and treatments of sulfur dioxide absorption have assumed instantaneous reactions (Part I). The Damkohler numer is large [$3.1 \cdot 10^9$, Equation (9)]. Also, as shown in Table 4, the boundary layer thickness δ_1 is approximately 10^{-3} when $Na_{tot} \geq 0.01$M. Since the film thickness is 1 mm, δ_1 is just over 1 μm. Yet, this thin layer causes a factor of 7 deviation from equilibrium flux. This result serves as a reminder that in the context of facilitated transport, reactions can be considered instantaneous only when the flux predicted by a nonequilibrium theory (for example, the NEBLA) agrees with the equilibrium theory.

TABLE 4. BOUNDARY LAYER THICKNESSES CALCULATED IN ANALYZING ALKALINE SOLUTION DATA

Na_{tot} mole/l	Entries are $10^2 \cdot \delta_1$ $10^6 \cdot y_{SO_2,0}$ 1 000	500	200	100
0.0	0.0183	0.0197	0.0216	0.0231
10^{-3}	0.0380	0.0439	0.0531	0.0613
10^{-2}	0.0906	0.1074	0.1274	0.1381
0.05	0.1280	0.1338	0.1380	0.1400
0.20	0.1240	0.1256	0.1279	0.1308
0.50	0.1178	0.1194	0.1234	0.1296
1.0	0.1116	0.1138	0.1201	0.1300
2.0	0.1014	0.1043	0.1128	0.1263

TABLE 5. BOUNDARY LAYER AND EQUILIBRIUM THEORIES COMPARED WITH WATER DATA

$10^6 \cdot y_{SO_2,0}$	$10^{10} \cdot \hat{N}$ moles $cm^{-2}s^{-1}$ $\hat{N}_{bl}$	$\hat{N}_{eq}$	$\hat{N}_{H_2O}$
1 000	12.8	11.8	11.9
500	8.52	8.41	8.44
200	5.06	5.17	5.32
100	3.43	3.61	3.81

An example is given in Table 5, where the flux through water predicted by the NEBLA (N_{bl}) and the equilibrium theory [Equation (30), Part I] is shown with the measured flux (Table 2). Besides agreeing with the data, the NEBLA agrees with N_{eq} to within 8%.

Because the NEBLA agrees with the water data and the alkaline solution data, the NEBLA is shown to be valid for all kinetic regimes for aqueous sulfur dioxide solutions. It would be useful to compare the NEBLA to data from other facilitated transport studies to see if it is valid for all kinetic regimes in other systems.

The potential gradient and the flux minimum: In dilute alkaline solutions, the potential gradient induces a concentration gradient in the alkali cation, Na^+. The approximate method of accounting for the potential (Part I) neglects this concentration gradient. The NEBLA underestimates the flux, therefore, when the potential gradient is nonzero and when Na^+ is the predominant cation ($2 \cdot 10^{-3}M \leq Na_{tot} \leq 0.03M$).

The potential gradient is also involved in producing the minimum in the flux near $Na_{tot} = 2 \cdot 10^{-2}M$. Addition of Na^+ reduces the effective diffusivity of the HSO_3^- ion as the potential gradient becomes less important [Equation (27), Part I]. Thus, although adding Na^+ increases the amount of HSO_3^- in solution, the HSO_3^- diffuses more slowly.

The pH changes that occur as Na^+ is added also have a role in producing the minimum. In these dilute solutions, HSO_3^- is the dominant sulfur carrier. Therefore, the concentration difference

$$C_{HSO_3^-}(0) - C_{HSO_3}(1)$$

is of primary importance [Equation (25), Part I]. The electroneutrality equation yields

$$C_{HSO_3^-}(0) - C_{HSO_3^-}(1) = C_{H_3O^+}(0) - C_{H_3O^+}(1) + 2[C_{SO_3^=}(1) - C_{SO_3^=}(0)] \quad (10)$$

(The OH^- concentration and the Na^+ concentration difference have been neglected (pH 3 to 6).) Consequently, in dilute solutions, where $SO_3^=$ is negligible, Equation (10) reduces to

$$C_{HSO_3^-}(0) - C_{HSO_3^-}(1) \simeq C_{H_3O^+}(0) \quad (11)$$

because $C_{H_3O^+}(1) << C_{H_3O^+}(0)$. In the dilute solution limit, then, the facilitation directly depends on the pH at $x = 0$ [pH (0)].

Addition of Na^+ causes pH(0) to increase which, according to Equation (11), causes the facilitation factor to decrease. The contribution of $C_{H_3O^+}(0)$ becomes small when Na^+ approaches 0.01M. Here, pH(0) $\simeq$ 4.

The facilitation would be eliminated unless the pH becomes high enough to create some $SO_3^=$. When $SO_3^=$ is present, the term

$$2[C_{SO_3^=}(1) - C_{SO_3^=}(0)] \quad (12)$$

can contribute to the flux. Since pK is 7.2 (25°C) for the reaction $HSO_3^- + H_2O \rightleftarrows SO_3^= + H_3O^+$, little $SO_3^=$ can be created near $x = 1$ until pH(1) approaches 7.

Thus, there is a window where pH(0) $\gtrsim$ 4, but pH(1) $\lesssim$ 7. In this window, the facilitation mechanism switches from being based on a direct pH difference to a pH induced $SO_3^=$ difference. The result is the minimum in the flux near $Na_{tot} = 2 \cdot 10^{-2}M$.

Effect of Film Thickness

Nonequilibrium theories predict that the facilitation factor changes with the film thickness. According to equilibrium theory, however, F is independent of L. To test for the thickness dependence, data at fixed $y_{SO_2,0}$ ($2 \cdot 10^{-4}$) and Na_{tot} (0.05M) were taken with film thicknesses between 0.37 and 4.8 mm. This range brackets the 1 mm film thickness used in the other alkaline solution experiments. Data are shown in Figure 9 with the data point from Figure 8*b* (L = 1 mm). The solid line is the NEBLA, and the dashed line is a sketch of the data.

The NEBLA agrees qualitatively with the data. The observed variation in F is a factor of 2.05, and the predicted variation is a factor of 2.47. The slopes of the theory and data curves are similar. In the previous discussion of the alkaline solution data, the NEBLA overpredicted the flux by ~30% when Na_{tot} = 0.05M (Figures 8*a*, *b*, *c*). The 20 to 40% overprediction in Figure 9 is therefore part of a systematic error in the NEBLA that is unrelated to the film thickness effect.

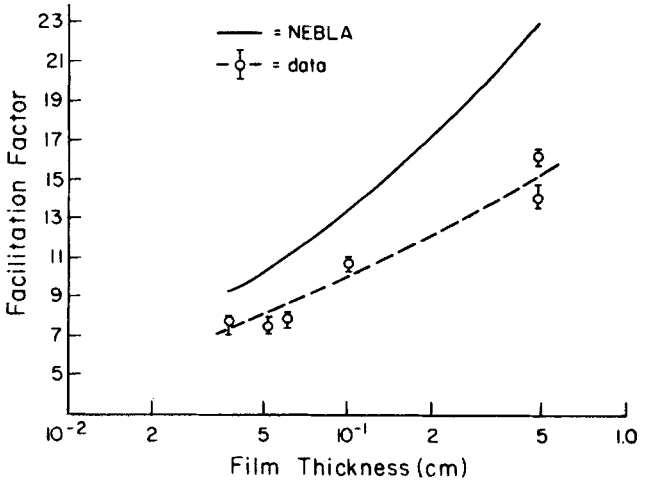

Figure 9. Variable film thicknesses. The facilitation factor changes with the film thickness. The NEBLA agrees qualitatively with the observed variation in F. Equilibrium theory predicts *F* independent of *L*. As *L* increases, *F* should approach the equilibrium value.

TABLE 6. BOUNDARY LAYER THICKNESSES IN VARIABLE FILM THICKNESS EXPERIMENTS

Data		Calculated by NEBLA	
L cm	F	$10^2 \cdot \delta_1$	$\hat{\delta}_1$ μm
$3.73 \cdot 10^{-2}$	7.78	0.3023	1.128
$5.11 \cdot 10^{-2}$	7.55	0.2356	1.204
$6.07 \cdot 10^{-2}$	7.93	0.2054	1.247
0.10	10.8	0.1380	1.380
0.476	14.1, 16.2	0.0396	1.885
F_{eq} = 77.6			

Since nonequilibrium effects are more important when the boundary layer is a larger fraction of the film thickness, δ_1 should increase as the observed facilitation factor decreases. This notion is confirmed by Table 6, where the facilitation factors from Figure 9 are given with L, δ_1 and $\hat{\delta}_1$. As F decreases, the boundary layer becomes a larger fraction of the film thickness. For the smallest thickness, δ_1 reaches its largest value, 0.3%. It is notable that $\hat{\delta}_1$ is relatively constant (1 to 2 μm).

ACKNOWLEDGMENT

This research was supported by the Pasadena Lung Association, the National Science Foundation (Energy Traineeship) and EPA grant No. R805736. The contents do not necessarily reflect the views and policies of the Environmental Protection Agency.

NOTATION

A = cross-sectional area of aqueous film
D_i = diffusion coefficient of species i
Da = Damkohler number, Equation (4)
F = facilitation factor; $(N-N_0)/N_0$
F_{SS} = facilitation factor derived from perturbation analysis of Suchdeo and Schultz (1974)
k_1, k_{-1} = forward and reverse rate coefficients for the reaction $SO_2(aq) + 2H_2O \rightleftarrows H_3O^+ + HSO_3^-$
K_1 = equilibrium coefficient for $SO_2(aq) + 2H_2O \rightleftarrows H_3O^+ + HSO_3^-$
L = thickness of aqueous film

M_d = molar flow rate of nitrogen through downstream side of cell
M_u = molar flow rate of nitrogen through upstream side of cell
N_i = flux of species i
N_0 = flux of sulfur dioxide in absence of chemical reactions
N_{H_2O} = flux of sulfur dioxide through water films
Na_{tot} = total alkaline sodium concentration (acid neutralizing capacity)
P_{tot} = total pressure
y_m = mole fraction of sulfur dioxide indicated by Meloy sulfur analyzer
$y_{SO_2,0}$, $y_{SO_2,1}$ = mole fraction sulfur dioxide in gas phase at $x = 0$ and $x = 1$

Subscripts

bl = boundary layer theory (NEBLA)
eq = equilibrium theory

Superscript

$\hat{}$ = dimensional variable or parameter

Greek Letters

γ_i = activity coefficient of species i
δ_0 = boundary layer thickness near $x = 0$
δ_1 = boundary layer thickness near $x = 1$
μ = solution viscosity
Φ = electric field potential

LITERATURE CITED

Bromley, L. A., "Approximate Individual Ion Values of β (or B) in Extended Debye-Huckel Theory for Uni-Univalent Aqueous Solutions at 298.15K," *J. Chem. Thermodynamics*, **4**, 669-73 (1972).

Chilcote, D. D., "The Diffusion of Ions in Agar Gel Suspensions of Red Blood Cells," PhD thesis, Calif. Inst. Technol. (1970).

Davies, C. W., *Ion Association*, Butterworths, Washington, D.C. (1962).

Eigen, M., K. Kustin and G. Maass, "Die Geschwindigkeit der Hydratation von SO_2 in wäBriger Lösung," *Z. Phys. Chem.*, **30**, 130-36 (1961).

Goettler, L. A., "The Simultaneous Absorption of Two Gases in a Reactive Liquid," PhD thesis, Univ. Del., Newark (1967).

Hetherington, P. J., "Absorption of Sulfur Dioxide into Aqueous Media," PhD thesis, Univ. Tasmania, Hobart (1968).

Hikita, H., S. Asai and T. Tsuji, "Absorption of SO_2 into Aqueous Sodium Hydroxide and Sodium Sulphite Solutions," *AIChE J*, **23**, 538-44 (1977).

Hikita, H., S. Asai and H. Nose, "Absorption of Sulfur Dioxide in Water," *ibid.*, **24**, 147-9 (1978).

Johnstone, H. F., and H. C. Blankmeyer, "Recovery of SO_2 from Waste Gases," *Ind. Eng. Chem.*, **30**, 101-9 (1938).

Onda, K., T. Kobayashi, M. Fujine and M. Takahashi, "Behavior of the Reaction Plane Movement in Gas Absorption Accompanied by Instantaneous Chemical Reactions," *Chem. Eng. Sci.*, **26**, 2009-26, 2027-35 (1971).

Phipps, R. L. "The Rate of Hydrolysis of Sulfur Dioxide," B.S. thesis, Mass Inst. Technol., Cambridge (1947).

Roberts, D. L., "Sulfur Dioxide Transport Through Aqueous Solutions," PhD thesis, Calif. Inst. Technol. (1979).

Schultz, J. S., J. D. Goddard and S. R. Suchdeo, "Facilitated Transport via Carrier-Mediated Diffusion in Membranes," *AIChE J*, **20**, 417-45; 625-45 (1974).

Standen, A., ed., *Encyclopedia of Chemical Technology*, 2 ed., Vol. 14, Wiley, New York (1962).

Suchdeo, S. R., and J. S. Schultz, "Mass Transfer of CO_2 Across Membranes," *Biochim. et Biophys. Acta*, **352**, 412-40 (1974).

Takeuchi, H., Y. Maeda and K. Itoh, *Kagaku Kogaku Ronbunshu*, **1**, 252 (1975); quoted by Takeuchi and Yamanaka, *Ind. Eng. Chem. Process Design Develop.*, **17**, 389-93 (1978).

Wang, J. C., and D. M. Himmelblau, "A Kinetic Study of Sulfur Dioxide in Aqueous Solution with Radioactive Tracer," *AIChE J*, **10**, 574-80 (1964).

Weast, R. C., *Handbook of Chemistry and Physics*, 52 ed., Chemical Rubber Company, Cleveland, Ohio (1971).

Manuscript received March 12, 1979; revision received January 17, and accepted January 23, 1980.

Aerosol Behavior in The Continuous Stirred Tank Reactor

JAMES G. CRUMP

and

JOHN H. SEINFELD

Department of Chemical Engineering
California Institute of Technology
Pasadena, California 91125

The basic features of aerosol behavior in the CSTR are examined. Solutions are obtained for the steady state aerosol size distribution during simultaneous coagulation, particle growth by vapor condensation and new particle formation by nucleation. Explicit distributions are shown for the case of a monodisperse feed aerosol.

SCOPE

Studies of particle formation and evolution in combustion systems and in laboratory simulations of atmospheric chemistry sometimes involve the use of a CSTR. The interpretation of aerosol size distributions in a CSTR requires the development and solution of the general population balance equation applicable to that system. The phenomena that must be considered include coagulation, particle growth by vapor condensation and new particle formation by vapor nucleation. Because the general problem of aerosol behavior in the CSTR does not appear to have been studied previously, an examination of the qualitative features of the steady state size distributions that may be achieved is deemed an appropriate first step to a more in depth analysis. Of particular interest is the elucidation of the effects of varying residence time and the characteristic times for coagulation and growth by condensation on the size distributions attained.

0001-1541-80-3904-0610-$00.75.